Tilt and Tamper Sensing UHF RFID Security Tag

M.A. Ziai, J.C. Batchelor

School of Engineering, The University of Kent, Cantebury, UK.
j.c.batchelor@kent.ac.uk

Keywords: RFID tag, Passive Sensing, Security.

Abstract

A passive tag is proposed for indicting mishandling of items in the supply chain. The tag signals excessive tilting by varying its read range and as a measure against counterfeiting, it is deactivated should it be removed from its original platform.

1 Introduction

While UHF Radio-frequency identification (RFID) technologies bring many benefits to automated parcel tracking [1], they do not sense if parcels have been mishandled by tilting, and also tags may be transferred to counterfeit items [2]. While delaminating tag labels reduce the risk of tag transfer in counterfeiting, it is still possible for the RFID transponder IC to be taken from the original tag and attached to a different antenna.

To address these issues, a totally integrated sensing tag is created for the following scenario. Initially, the tag has a very short read range when it is attached to a parcel and the tag EPC code is set and logged using a handheld reader. After mounting on the parcel, the tag read range is maximum for reliable detection by readers several metres away. Should the parcel be tilted, the tag read range falls to around half of the maximum value. The reduced read range indicates a tilt event has occurred prior to the read. If the tag is removed from the parcel, the transponder IC is ripped from its pins and the tag is rendered useless.

2 Tag Mechanisms

To enable passive operation and the memorization of state occurrences, the tag uses integrated mechanical mechanisms as illustrated in Fig. 1. The antenna is suspended a distance h_1 above a conducting ground and mount detection is enabled by adjusting h_1 between two discrete values (0.5mm before mounting, and 5 mm when mounted). The detuning that occurs between the 2 values affects the RFID read range and this signals if the tag is mounted.

Tag removal, or tamper detect is achieved through a clip-lock attachment that directly fixes the transponder IC to the inside of the top cover. The RF pins of the SOT-232 package are soldered to the antenna terminals and before mounting, the chip is separate from the top cover. When mounted on a surface, the antenna substrate is pushed against the springs and the IC becomes clip-locked to the inside of the cover. If the tag is subsequently unmounted, the springs push the substrate from the upper cover but the IC remains within its clip-lock. The spring separating force breaks the IC pins from the SOT package and the chip is rendered unusable.

Tilt detection is achieved through the incorporation of two rectangular pads with the antenna port as shown in Fig. 1(b). When the tag is tilted a conducting disk drops through a routed channel in the cover. The disk ends up in close proximity to the antenna pads and the capactive loading detunes the antenna in a controlled way.

3 Antenna Design

The tag antenna in Fig. 2 is a coplanar feed half wave dipole on FR4 dielectric. It differs from other embedded T-matched designs [3] through its multilayer substrate, incorporated sensing pads and rear ground plane. Fig. 2(c) shows the transponder chip connection and the inset sensing pads.

The antenna length was initially calculated from:

$$L_1 = 0.47 \cdot \frac{c}{f_{res}\sqrt{\varepsilon_{re}}} \qquad (1)$$

where f_{res}, is the resonance frequency and ε_{re} is the effective relative permittivity of the substrate and air layers between the antenna and the ground plane. Since the conducting ground is only 13% larger than the antenna, the structure resembles a parallel plate capacitor and the ε_{re} of the material stack is calculated from [3]:

$$\varepsilon_{re} = \varepsilon_{sub} \frac{\left(\varepsilon_{air} + \frac{h_1}{h_2}\right)}{\left(\varepsilon_{air} + \varepsilon_{sub} \cdot \frac{h_1}{h_2}\right)} \qquad (2)$$

In the mounted state (h_1 = 5mm), the antenna was tuned for maximum power transfer with a conjugate match to the RFID chip by adjusting slot dimensions L_2 and S together with the feed line width W_2.

The ground plane isolates the tag from the mounting surface and moves between 2 discrete h_1 separations from the antenna to signal that the tag is either in an unmounted, or mounted state. The distinct state based approach is used to avoid inaccuracies in exact ground plane positioning. It is therefore necessary to establish the antenna performance as a function of ground plane separation.

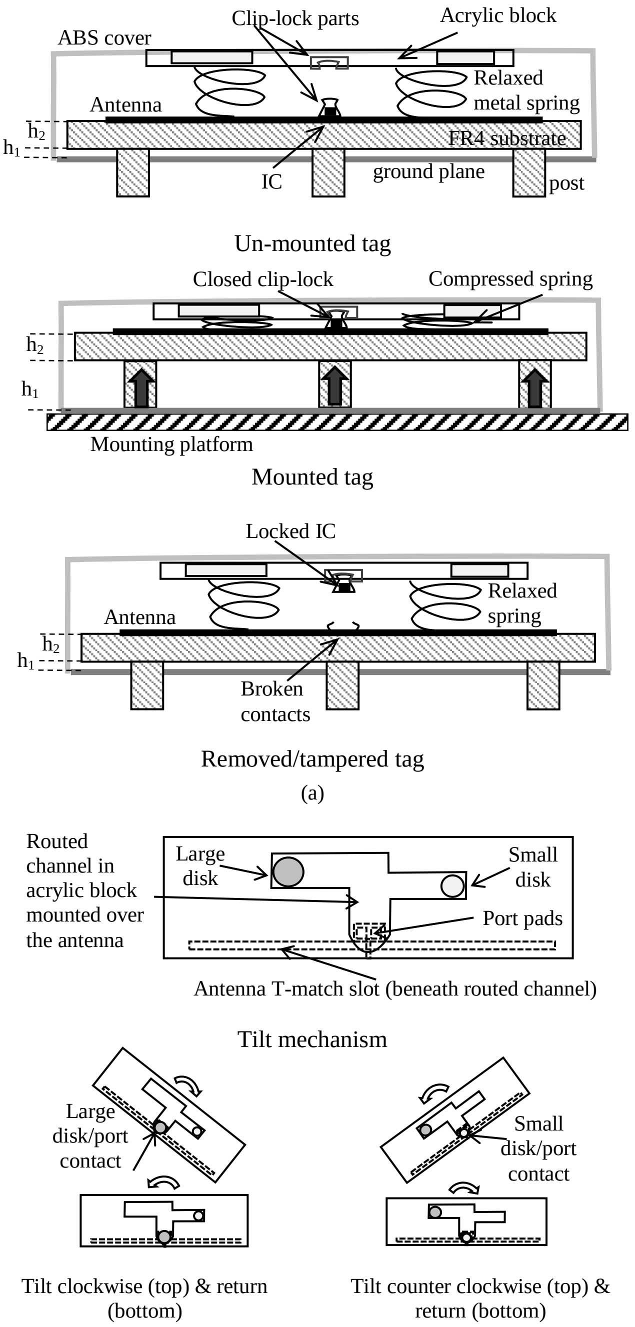

Fig. 1. Passive tag mechanical sensing mechanisms. (a) Mounting sensor & Tamper detecting mechanism (side view), (b) Tilt detect and memory mechanism (top view).

For small h_1 values the proximity of the ground plane causes a reduction in radiation resistance and high input reflection loss. Simulated resonance frequency and total efficiency for varying ground plane separation identified the optimal h_1 to be 5 mm. Therefore, h_1 values of 0.5 mm and 5 mm were chosen to give the maximum variation in read range from before the tag is mounted, to when it is attached.

The antenna, enclosed in its ABS casing, was simulated with CST MWS® to tune to the American UHF RFID band, resulting in the dimensions in Table 1. Removal of the casing caused 62 MHz detuning, with marginal change in the tag performance. The metal springs were found to have no significant effect on the antenna gain (5.9 dBi) or total efficiency (78%), where the latter includes radiation, material, and input losses.

Parameter	(mm)
Ground plane L × W	155 × 42
Dipole $L_1 \times W_1$	134 × 35
Slot $L_2 \times S$	109 × 3
Feed line length W_2	3
Pad $L_3 \times W_3$	3.5 × 3.5
Pad recess, L_4 & W_4	10 & 4
Air gap height, h_1	0.5 , 5
FR4 substrate height, h_2	1

Table 1: Tag dimensions (f_{res} = 915 MHz).

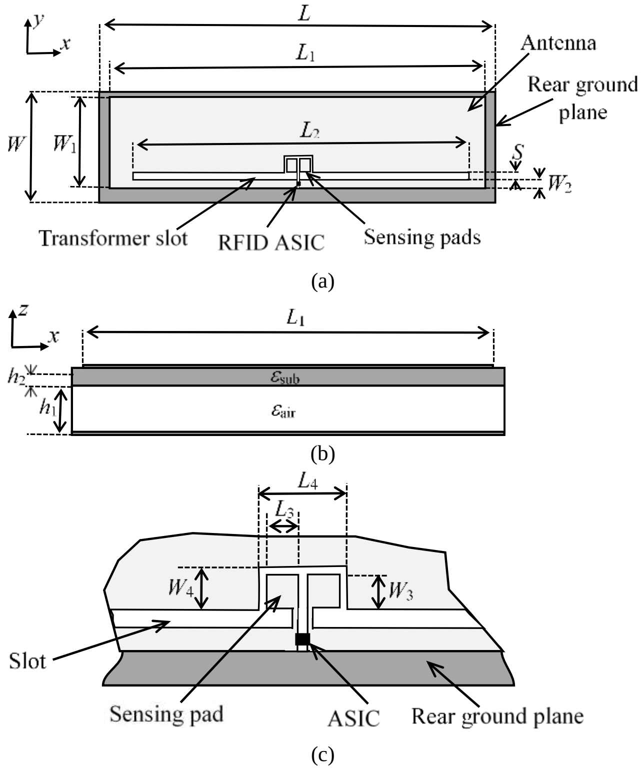

Fig. 2. (a) Tag antenna geometry, (b) side view, (c) close view of feed and tilt sensor pads. Dimensions are given in Table I.

4 Antenna Parametric Analysis

To establish a design guide for input match at h_1 = 5 mm, the tag was simulated for various values of slot width S. Fig. 3(a) shows how the real part of the antenna impedance decreases for wider slots, and the reactance becomes less inductive. S = 3 mm is selected to provide the required inductance at the antenna port to conjugate match an Alien Higgs 3 chip (Z_{ic} = 25 - j149 Ω) [4].

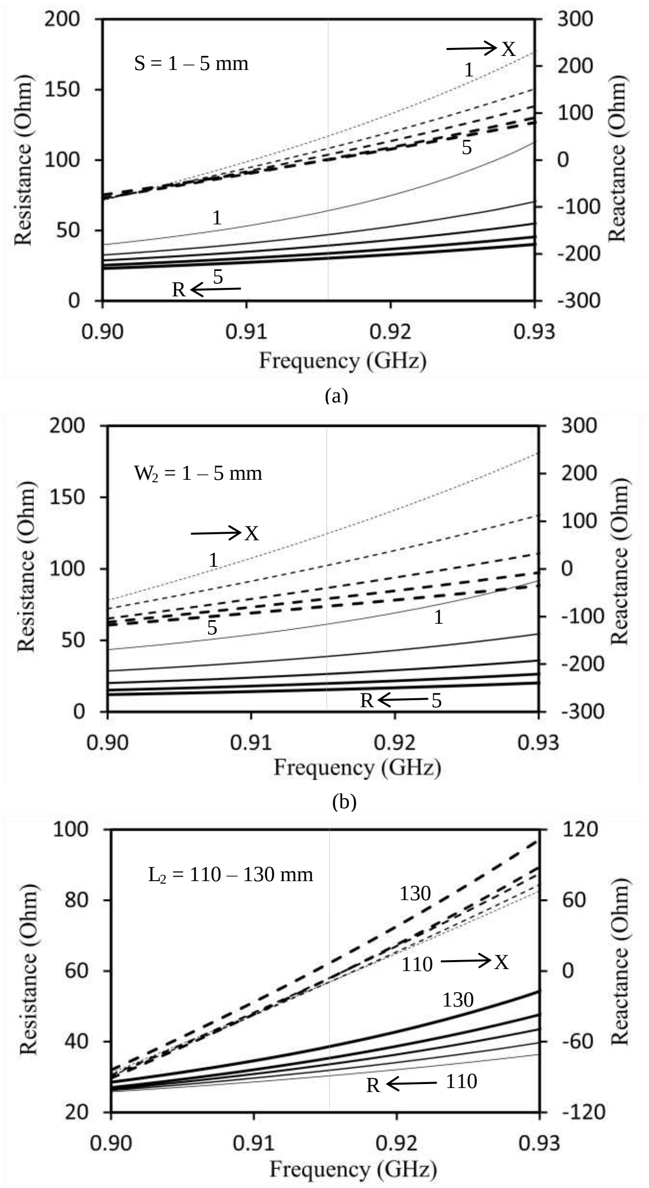

Fig. 3. Simulated real and imaginary antenna port impedance normalized to X_{ic} = – j149 Ω for (a) slot width S of 1 – 5 mm, (b) stub width W_2 of 1 – 5 mm, (c) stub length L_2 of 110 – 130 mm. Solid lines = R, dashed line = X.

Variation of feed width in Fig. 3(b) shows that while W_2 = 1 or 2 mm provides sufficient inductance, the impedance varies significantly between 905 and 928 MHz making the design narrowband. Therefore, W_2 = 3 mm was selected where the impedance variation with frequency is lower. The slot length L_2 has little effect on reactance as shown in Fig. 3(c) and was set to 110 mm to match the chip resistance. After tuning, the port resistance does not change significantly across the American RFID bands (905 -928 MHz), while the inductive reactance changes by about 100 Ω. The tag total efficiency has values of -5, -0.8 and -7 dB at the lower band, the resonance frequency and the upper band respectively.

5 Tilt Sensing by Antenna Impedance Mismatch

Fig. 4 shows the simulated surface currents for the tag before it is mounted, and when it is mounted on metal, first un-tilted, then tilted. The low surface current before mounting, Fig. 4(a), is due to the proximate rear ground plane. After mounting the tag is well matched and strong surface currents are observed in Fig. 4(b). However, a noticeable reduction in current magnitude is observed in Fig. 4(c) after tilting as the tag is now partially mismatched.

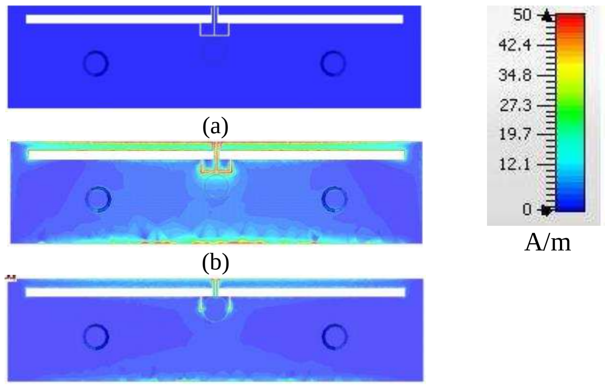

Fig. 4. Tag antenna surface current at 915 MHz on (a) no mount (h_1 = 0.5 mm), (b) metal plate (h_1 = 5 mm) – no tilt, (c) tilted.

The effect on tag performance for these states can be appreciated by considering the read range d [5]:

$$d \le \frac{\lambda}{4\pi}\sqrt{EIRP \times G_{tag} \times \tau / P_{th}} \quad (3)$$

where EIRP is the reader effective isotropic radiated power, G_{tag} is the tag antenna gain and P_{th} is the chip turn-on power. The power transfer coefficient τ between the antenna and the chip is related to the voltage reflection coefficient Γ of the tag antenna port by [6]:

$$\tau = 1 - |\Gamma|^2 = 4R_{ic}R_{ant}/|Z_{ic} + Z_{ant}|^2 \quad (4)$$

where Z_{ic} and Z_{ant} are of opposite reactance types and represent the complex port impedances of the transponder chip and the antenna respectively, while R_{ic} and R_{ant} are the corresponding real parts. The voltage reflection coefficient is [7]:

$$\Gamma = (Z_{ic}^* - Z_{ant})/(Z_{ic} + Z_{ant}) \quad (5)$$

Tilt detection is achieved by the sensing pads in Fig. 2(c). The pads are open circuit when the tag is un-tilted and the pad impedance Z_1 is connected in parallel with the antenna port impedance. However, when the tag is tilted beyond a predefined angle, a metallic disk with a thin polymer coating makes capacitive contact with the pads causing the impedance Z_2 to appear across the antenna port. From (5), the port voltage reflection coefficient is given by:

$$\Gamma = \left(Z_{ic}^* - \left(\frac{Z_{ant}Z_{1,2}}{Z_{ant}+Z_{1,2}}\right)\right) / \left(Z_{ic} + \left(\frac{Z_{ant}Z_{1,2}}{Z_{ant}+Z_{1,2}}\right)\right) \quad (6)$$

where $Z_{1,2}$ represents the impedance of the open circuit pads and the pads + disk respectively.

	C, L	R (Ω)	X (jΩ)	|Γ| from (5)	d (m) from (3)
Antenna alone (Z_{ant})	19 nH	25	110		
Sensing pad (un-tilted: Z_1)	0.35 pF	0.52	-492		
Sensing pad (Tilted: Z_2)	1.02 pF	0.06	-169		
Antenna & pads (un-tilted)	27 nH	56	155	0.42	17
Antenna & pads (tilted)	36 nH	212	202	0.79	11

Table 2: Simulated sensor pad effect on tag port impedance, calculated reflection coefficient, and RFID read range. Platform = air with tag activated (h_1 = 5 mm, frequency = 915 MHz, reader EIRP = 36 dBm, G_{tag} = 5.7 dBi, and P_{th} = - 15 dBm.

The un-tilted tag is designed for maximum power transfer so $\Gamma_{un\text{-}tilted}$ has a low magnitude. When tilted, the mismatch associated with Z_2 in (6) results in a higher magnitude for Γ_{tilted}. Table 2 gives the simulated impedances respectively for Z_{ant}, Z_1 and Z_2. Port values are also given for the connected antenna and pad impedances in both states together with the corresponding reflection coefficients calculated from (5). Read range values obtained from (3) are also given. It can be seen that the tilted read range falls to half of the un-tilted value, and it is this significant difference that allows discrimination between the un-tilted and tilted states.

6 Measured Tilt Signalling

The fabricated tag is shown in the tilted (Fig. 5(a)), and tampered states (Fig. 5(b)). The read range d was measured from 800 to 1000 MHz using Voyantic equipment [8].

The read ranges at 915 MHz for the initial (un-mounted), mounted (on metal) and tilted (on metal) states were 1.1, 20.3 and 7.5 m respectively with sufficient bandwidth to cover the American RFID band. In the tilted state, the read range decreased by 63% with less than 10 MHz shift in the peak frequency. This demonstrates good discrimination between the states. In the initial state, the tuned frequency decreased by more than 70 MHz giving a measured read range of 1 m in the tag deployment stage where a handheld reader is used.

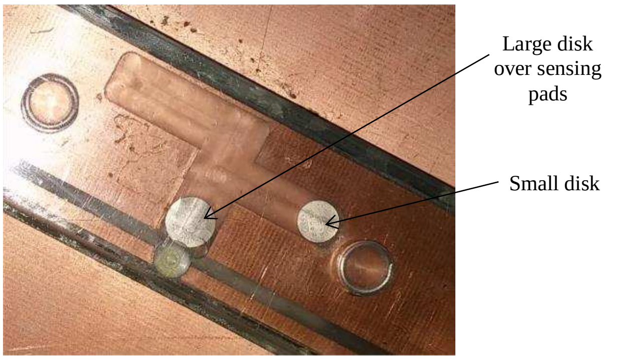

(a)

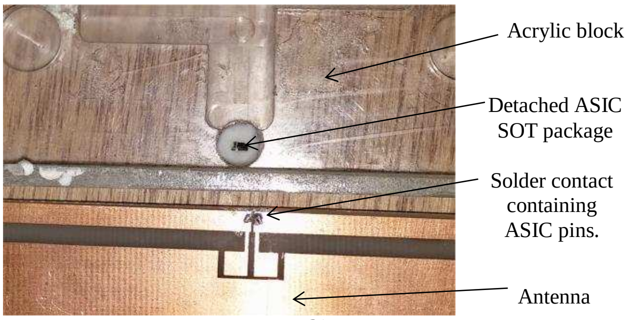

(b)

Fig. 5. Prototype tag (a) tilted state and (b) tampered (removed from platform).

7 Conclusions

A rugged cased tag is described for tamper and tilt sensing on different platforms, where the use of a stud-lock system attached to the tag ASIC prevents fraudulent swapping of transponders to counterfeit tag antennas. Discrete state antenna impedance detuning due to the interaction of conducting discs passively memorises inappropriate tilting events.

References

[1] I.P. Vlachos, "A hierarchical model of the impact of RFID practices on retail supply chain performance", Expert Systems with Applications, 41, (1), pp. 5-15, (2014).

[2] S. Mohite, G. Kulkarni, R. Sutar, "RFID security issues", International Journal of Engineering Research & Technology (IJERT), **2**, (9), pp. 746-748, (2013).

[3] G. Marrocco, "The art of UHF RFID antenna design: impedance-matching and size-reduction techniques", IEEE Antennas Propag. Mag., **50**, (1), pp. 66-79, (2008).

[4] D. Guha, Y.M.M. Antar, "Microstrip and printed antennas: new trends, techniques and applications'" (New York, Wiley, 2010).

[5] Alien HiggsTM-3 datasheet, www.alientechnology.com, accessed April 2017.

[6] K. Finkenzeller, "Physical Principles of RFID systems", RFID Handbook: Fundamentals and Applications in

Contactless Smart Cards and Identification (Wiley, 2010, 3rd edn.).
[7] K.V.S. Rao, P.V. Nikitin, S.F. Lam, “Impedance matching concepts in RFID transponder design”, Proc. 4th IEEE Workshop on Automatic Identification Advanced Technologies (AutoID 2005), Buffalo, NY, pp. 39-42, (2005).
[8] “Voyantic Ltd. Tagformance: Measurement and testing solutions for the RFID industry and academia”, http:// voyantic.com/products/tagformance-pro, accessed April 2017